Advanced Materials Research *Online: 2011-04-19*
ISSN: 1662-8985, Vol. 223, pp 162-171
doi:10.4028/www.scientific.net/AMR.223.162

On methodologies inside two different commercial codes to simulate the cutting operation

Yancheng Zhang[1,a]*, Domenico Umbrello[2,b], Tarek Mabrouki[1,c], Stefania Rizzuti[3,d], Daniel Nelias[1,e], Yadong Gong[4,f]

[1] Université de Lyon, CNRS, INSA-Lyon, LaMCoS, UMR5259, F69621, France

[2] University of Calabria, Department of Mechanical Engineering, 87036 Rende (CS), Italy

[3] Politecnico di Torino, DISPEA, 10129 Torino, Italy

[4]School of Mechanical Engineering & Automation, Northeastern University, Shenyang, 10004, China

[a]*yancheng.zhang@insa-lyon.fr, [b]d.umbrello@unical.it, [c]tarek.mabrouki@insa-lyon.fr,

[d]stefania.rizzuti@polito.it, [e]daniel.nelias@insa-lyon.fr, [f]gongyd@mail.neu.edu.cn

Keywords: Cutting, Finite Element Method (FEM), Ti6-Al-4V

Abstract. Nowadays, numerical simulation of cutting processes receives considerable interest among the scientific and industrial communities. For that, various numerical codes are used. Nevertheless, there is no uniform standard for the comparison of simulation model with these different software. So, it is often not easy to state if a given code is more pertinent than another. In this framework, the present work deals with various methodologies to simulate orthogonal cutting operation inside two commercial codes Abaqus and Deform. The aim of the present paper is to build a common benchmark model between the two pre-cited codes which can initiate other numerical cutting model comparisons.

The study is focused on the typical aeronautical material - Ti-6Al-4V - Titanium alloy. In order to carry out a comparative study between the two codes, some similar conditions concerning geometrical models and cutting parameters were respected. A multi-physic comprehension related to chip formation, cutting forces and temperature evolutions, and surface integrity is presented. Moreover, the numerical results are compared with experimental ones.

Introduction

Finite element modeling (FE Modeling) of metal machining has been recently received considerable interest during the past thirty years, and lots of research works [1, 2] have been published since the pioneering studies by Usui and Shirakashi [3]. It is known that finite element method (FEM) provides precise information concerning variables like plastic strain, strain rate or stress distributions during tool-workpiece interaction which are difficult to measure experimentally. Consequently, with this numerical method, a general understanding of chip formation process [4] can be improved. More knowledge about the chip genesis phenomenon can be deduced as FEM takes into account both material thermo mechanical behavior and contact non-linearity and it results to be more accurate than analytical models [5].

Despite some limitations and constraints, as well as difficulties in identification of input parameters, lack of robustness in some quantitative results and so on, numerical simulations can be considered promising to study cutting process and potentially allowing to reduce the experimental cost [6].

In the recent years, researchers tried to find the common FEM and simulation parameters for different FE software and metal materials [6 - 8]. Deshayes et al. [7] have carried out a FEM comparison study dealing with the cutting of (AISI) 4340 steel alloy with AdvantEdge and Abaqus/Explicit, obtained results were qualitatively in agreement with experimental ones. Similar simulation, with the two pre-cited software, was also performed by Arrazola et al. [6] in the case of AISI-4140 steel alloy machining. Soriano and Lianos et al. [8] have presented a comparison of 3D machining mod-

els developed under commercially available FE software Abaqus/Explicit, AdvantEdge and Deform3D for the work material Inconel 718, Computational results obtained from the FE models treating the effect of cutting speed on part-too interaction were presented.

In this general framework, the benchmark objective is to compare predictions on Ti-6Al-4V Alloy cutting simulation when different codes are set in their best prediction. It should be noticed that the elaboration of benchmark, insight the two pre-cited codes, is based on the optimal conditions for each of them in terms of material laws, damage criteria, etc. This will help scientific community to get precise information for other numerical cutting model comparisons. This paper is composed of three main parts:

First, some aspects concerning the material properties are briefly discussed.

Then, the numerical model set up in Abaqus/Explicit™ (v6.7) and Deform-2D™ (v10.1) are described briefly.

Finally, the experimental and numerical plan results are detailed. Results are discussed and overall conclusions are pointed out.

Material Aspects and Modeling of Ti-6Al-4V alloy

Ti-6Al-4V has good specific strength, toughness and corrosion resistance which makes it attractive for applications in aerospace, pressure vessels, surgical implants, etc. Components for these applications have precise requirements on mechanical and physical properties [9]. The chemical composition and the key physical and mechanical properties of Ti-6AL-4V are listed in Table 1 and plotted in Fig. 1.

Table 1: Chemical, mechanical and physical properties of the Ti-6Al-4V [10]

Description	Values
Al	5.50 – 6.75
C	<= 0.0800
H	<= 0.0150
Fe	<= 0.400
N	<=0.300
O	<= 0.200
Ti	87.725 - 91.0
V	3.50 - 4.50
Other, each	S<0.0500
Other, total	<= 0.300
Young's modulus	210 GPa
Poisson ratio	0.3
Mass density [kg/m^3]	4430
Specific heat [J/kg/°C]	(See Fig. 1.a)
Thermal conductivity [W/m/°C]	(See Fig. 1.b)

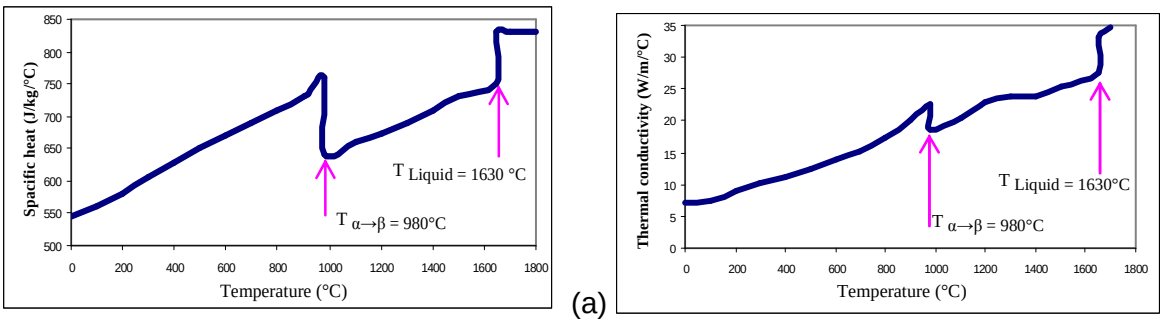

(a) (b)

Fig. 1: Physical properties of the Ti-6Al-4V alloy as a function of temperature: (a) specific heat and (b) thermal conductivity [11].

Finite Element Modeling

In order to build a common FE-model for chip formation process during orthogonal cutting process, ABAQUS/EXPLICIT-2D and DEFORM/IMPLICIT-2D software have been exploited.

Abaqus/Explicit™: Model features. The general-purpose FEA software Abaqus/Explicit™ (v6.7) has been exploited to set up the FEM in two dimensions (2D). For the present contribution, the 2D orthogonal cutting model was developed as shown in Fig.2. Linear quadrilateral continuum plane strain element CPE4RT with reduced integration was utilized for a coupled temperature–displacement analysis. To optimize the contact management during simulation, a multi-part model (Fig. 2) was typically developed with four geometrical parts.

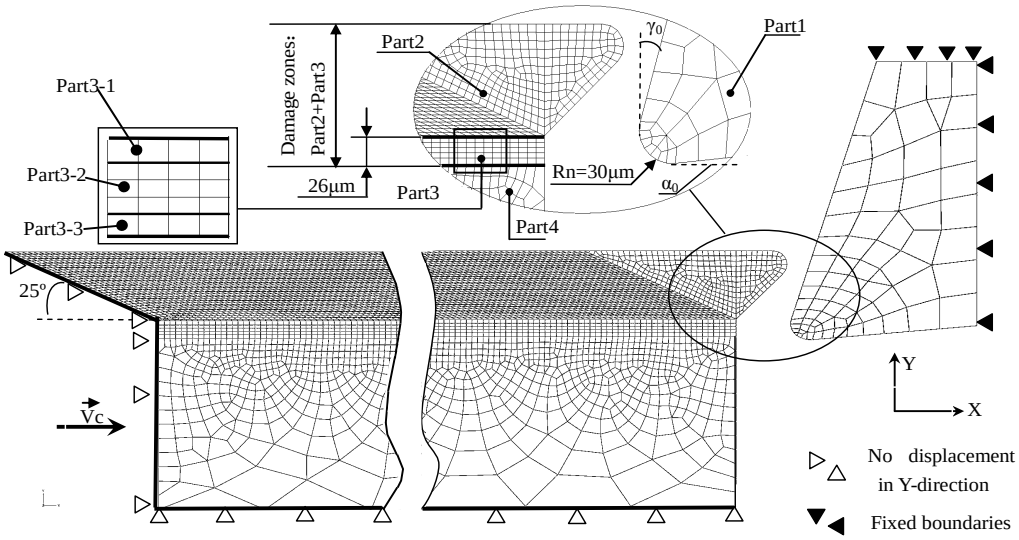

Fig. 2: Model mesh and boundary conditions.

The material constitutive model of Ti-6AL-4V and damage initiation was presented by the Johnson-Cook (J-C) one [12, 13], while the Hillerborg's fracture energy [14] was introduced to model damage evolution with the form of linear and exponential for the sacrificial layer (part 3 –Fig. 2) and chip zone (part 2), respectively.

The scalar stiffness degradation for the linear damage process used for part 3 is given by:

$$D = \frac{L\bar{\varepsilon}}{\bar{u}_f} = \frac{\bar{u}}{\bar{u}_f} \tag{1}$$

In the above equations L, $\bar{\varepsilon}$ *and* $\bar{u}$ *are* the element characteristic length, the equivalent plastic strain, and the equivalent plastic displacement. Where the failure equivalent displacement is $\bar{u}_f = 2G_f / \sigma_Y$, G_f is the fracture energy dissipated during the damage evolution process and σ_Y is the yield stress at damage initiation. Whereas an exponential damage parameter used for part 2, evolves according to:

$$D = 1 - \exp\left(-\int_0^{\bar{u}} \frac{\bar{\sigma}}{G_f} d\bar{u} \right) \tag{2}$$

The scalar stiffness degradation, D, approaches to one asymptotically at an infinite equivalent plastic displacement.

From the aspect of contact mechanics [15], the improved zorev's friction contact model was implemented to resolve element distortion on chip contact surface.

It should be noticed that the thermal conductance at tool-chip interface was kept as a constant value of 46000 W/m^{2}K [16].

Deform/Implicit™: Model features. Parallel to the cutting simulations performed with Abaqus, the Software DEFORM2D^{TM}, which is based on an implicit Lagrange formulation was also applied for the case of cutting study.

A FE model in plane strain coupled thermo-mechanical analysis was performed in orthogonal cutting conditions. This model was composed of the workpiece and the tool. The workpiece was meshed with isoparametric quadrilateral elements and modelled as elasto-plastic, while the tool was considered as a rigid body. The work material behaviour for Ti-6Al-4V was modelled using the flow stress developed by SFTC and implemented in DEFORM's library [17].

According literature, the chip segmentation can be considered as a consequence of the fracture process taking place during chip formation. Other phenomena, such as thermal softening can coexist with fracture to participate to segmentation genesis. In this research, Cockroft and Latham's fracture criterion [18] was used, to predict the effect of the stress on the chip segmentation during orthogonal cutting. Cockroft and Latham's criterion is expressed as:

$$\int_0^{\bar{\varepsilon}_f} \sigma_1 d\bar{\varepsilon} = C \tag{3}$$

where ε_f is the effective strain, σ_1 principal stress and C the material constant representing resistance to failure (sometimes called "damage value"). Cockcroft & Latham's criterion says that when the integral of the left term (applied state) in Eq. 3 reaches the value of C (material state), the fracture occurs and the chip segmentation starts. In this work, C was set equal to 240 MPa.

As far as friction modeling is concerned, a simple model based on the constant shear hypothesis was implemented in the FE code, with the shear factor kept at m = 0.6 considering as dominant the phenomena appearing in the sticking zone, in which this model is effective.

It is worth pointing out that the global heat transfer coefficient at the tool-chip interface, h, was fixed equal to 100000 kW/m^{2}K, assuming contact is thermally perfect under high cutting pressures [19].

In Fig. 3, the mechanical and thermal boundary conditions of the 2D finite element model are schematically shown.

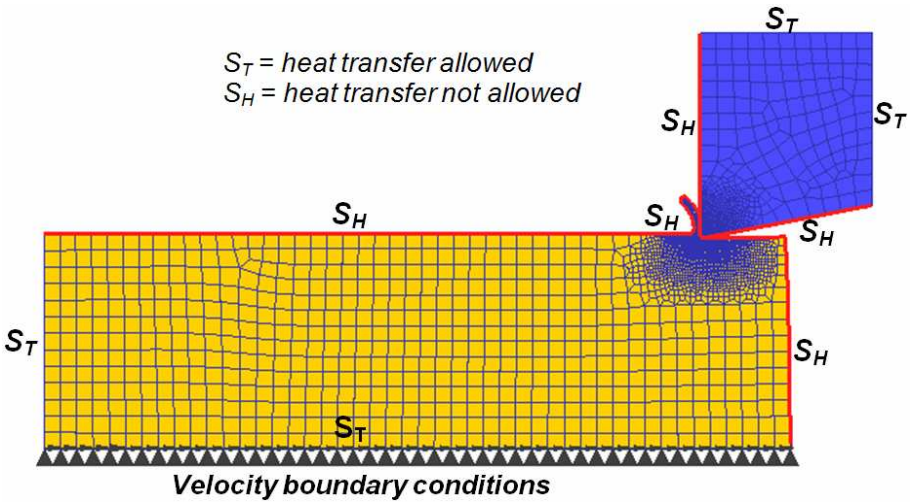

Fig. 3: 2D numerical model set up (Deform /Implicit 10.1).

Simulation results and discussion

Three numerical tests were carried out to evaluate the robustness of the two simulation models. Also, a comparison between computed results and experimental tests selected from literatures [13, 20-22] were done. The first group is mainly focused on studying the physical phenomenon accompanying cutting process with positive rake angle of the cutting tool. The second group concerns the cutting with the negative rake angle, and the third group aims to investigate the influence of tool wear on the residual stress distribution on the machined surface. The cutting conditions are resumed in Table 2.

Table 2: Process parameters employed in the study

Cutting parameters		Group I [20, 21]	Group II [22]	Group III [13]	
				III-1	III-2
Cutting speed (Vc), [m/min]		120	180	320	320
Uncut chip thickness, [mm]		0.127	0.1	0.1	0.1
Depth of cut, [mm]		2.54	2	1	1
Cutting edge radius, [μm]		30	20	sharp	sharp
Rake angle, [deg]		15	-4	5	5
Clearance angle, [deg]		6	7	8	8
Flank wear, [mm]		—	—	0.03	0.2
Experimental Results					
Forces	Cutting force: F_c [N]	559	548	—	—
	Thrust force: F_t [N]	—	—	—	—
Chip morphology	Chip peak: h_1 [μm]	165	131	—	—
	Chip valley: h_2 [μm]	46	62	—	—
	Chip pitch: L_1 [μm]	140	100	—	—
	Chip compression ratio: CCR	1.30	1.31	—	—

Cutting force evolution and chip morphology. Table 3 shows the computed results based on both Abaqus and Deform simulations. Results concern the chip morphologies in terms of measured lengths characterising a chip segment shape (valley, pick and pitch) in the two pre-cited group conditions (as presented in Fig. 4). Also it is demonstrated in the same conditions the extracted cutting force, thrust forces. All results are compared with experimental ones for group I and group II, while the simulation results from group III can be used as the qualitative comparison for the two different software.

A general overview of the results allows to establish that lower errors can be obtained with the utilized Abaqus set up. Anyway, going to details, some considerations have to be drawn. As far as cutting force is concerned, it is worth pointing out that even if it is well predicted by Abaqus, from a qualitatively point of view Deform allows to better describe the evolution of thrust force, even if it is not possible to compare the numerical values with the experimental ones. Globally, it is important to note that the two codes allow a very interesting prediction regarding experimental ones. Finally, analyzing the errors obtained in the predictions of the chip morphology, it is possible to state that from a numerical point of view, Abaqus provided the lowest errors in most of the cases. Concerning the chip formation process, it is worth to underline that in Abaqus the chip segmentation is the result of a thermal softening state. On the other hand, when the software Deform is utilized, the chip formation is obtained by implementing Cockroft and Latham's criterion, thus allowing to predict the effect of tensile stress on the chip segmentation during orthogonal cutting.

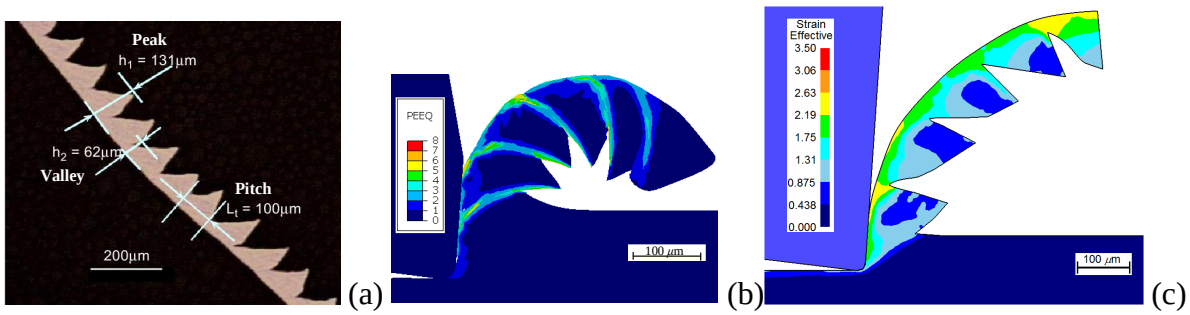

Fig. 4: Chip morphology obtained at V_C = 180 m/min, f = 0.1 mm/rev: (a) Experimental chip [22]; Equivalent plastic strain computed with (b) Abaqus/explicit and (c) Deform/implicit

In addition, in Deform, the element deletion feature was also applied in these numerical simulations to better describe the chip fracture instead of the remeshing–rezoning methodology. This choice appears particularly suitable for describing the physics of crack initiation and propagation during chip formation of Ti-6Al-4V alloy. In fact, as observed by diverse authors [17], the crack which determines the serrated chip during cutting Ti-6Al-4V, always occurs in the primary shear zone on the tool tip side. This is due to the fact that in this region the maximum principal stress and shear stress are located. Shear stress concerns the shear plane zone and tensile stress facilitates the initiation of the crack.

Table 3: Numerical effects obtained after the sensitivity analysis with two FE – Codes

Simulation Test			Cutting forces		Chip morphology parameters				Workpiece	Tool
			F_c	F_t	h_1	h_2	L_1	CCR	θ_{WT}	θ_{TT}
ABAQUS	GI_Vc_120		541.3	39.0	161.5	48.0	133.0	1.27	591-689	486-631
	Error with experimental values (%)		-3.17		-2.12	4.35	-5	-2.12		
	GII_Vc_180		580.0	164.5	132.0	77.0	96	1.32	754-919	462-611
	Error with experimental values (%)		5.8		0.76	24.19	-4	0.76		
	GIII_Vc_320	Wear_0.03	166.5	21.0	131.2	34.0	96.0	1.31	631-693	514-580
		Wear_0.2	186.9	40.4	131.7	31.2	96.0	1.32	629-699	541-603
DEFORM	GI_Vc_120		508.9	305.4	152	42	133	1.20	678-781	621-707
	Error with experimental values (%)		-8.96		-7.88	-8.70	-5.00	-7.69		
	GII_Vc_180		501.1	270.9	155.5	47.8	121.0	1.55	820-934	672-766
	Error with experimental values (%)		-8.56		18.70	-22.90	21	18.32		
	GIII_Vc_320	Wear_0.03	228	101	157	34.1	214.5	1.57	805-918	793-903
		Wear_0.2	267	111	190.5	54	221.5	1.905	819-933	817-932

F_c [N]: Cutting force. F_t [N]: Thrust force. CCR: Chip compression ratio.
h_1 [µm]: Chip peak. h_2 [µm]: Chip valley. L_1 [µm]: chip pitch.
θ_{WT} [°C]: Maximum temperature on workpiece θ_{TT} [°C]: Maximum temperature over tool rake surface.

Temperature distribution due to tool wear. To analyze the influence of tool wear on temperature distribution, the computation of temperature distribution beneath the machined surface was studied in group III. The flank wears size of cutting tool are considered as the initial state and kept constant during the simulation test. The tools' geometry shapes with flank wear are illustrated in Fig. 5. Two numerical comparisons were done in order to highlight the difference and/or the similarity between Abaqus and Deform software: (i) temperatures comparison on machined surface and sub-surface near the tool tip for different flank wear; (ii) Temperatures comparison along the primary and secondary shear zones, highlighting the difference between maximum ones.

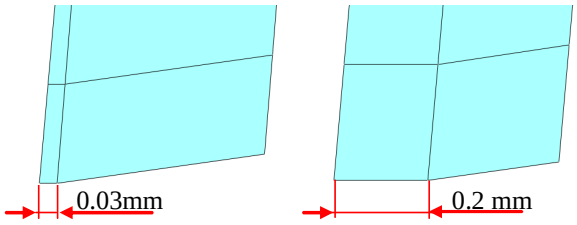

Fig. 5: Tool shapes with flank wear.

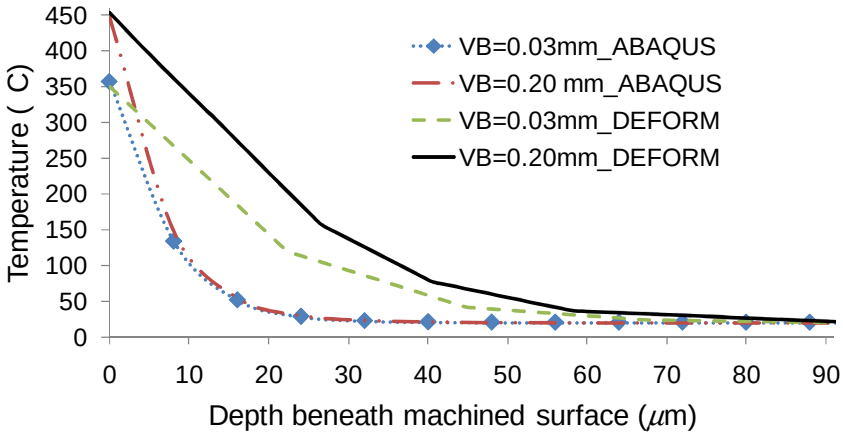

Fig. 6: Temperature depth profile beneath the machined surface.

Fig. 6 shows as both Deform and Abaqus predict similar temperature values on the machined surface. Furthermore, for a given code numerical results present a temperature gradient about 90°C for the two flank wear lengths at the generated surface. Therefore, both Deform and Abaqus take into account the heat generated along the flank face/workpiece interface due to modelled flank wear. In contrast, there is some discrepancy in temperature prediction below the machined surface (Fig. 6) since for both modelled tool flank wears, Deform shows higher temperature than Abaqus. The reason is related to the different heat global coefficient and interface thermal model used and implemented in the two softwares.

What's more, the temperature distribution in the whole cutting model is presented in Fig. 7. It can be noted that there is a disagreement concerning temperature distribution given by Abaqus and Deform. Also, it is underlined a non concordance in the chip morphologies. Indeed, the chip segmentation morphology obtained by Abaqus is the result of a thermal softening state (due to plastic localization in the primary shear zone, followed by a damage state presented by the material stiffness degradation). The temperature given by Deform modeling is higher at the secondary shear zone and this due to the fact that the contact is considered perfect at tool-chip interface.

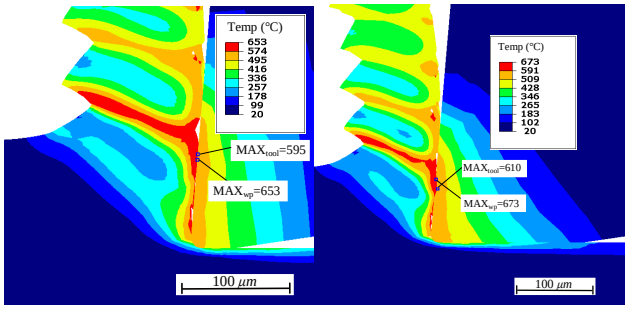

Abaqus: (a) VB=0.03mm; (b) VB=0.20mm.

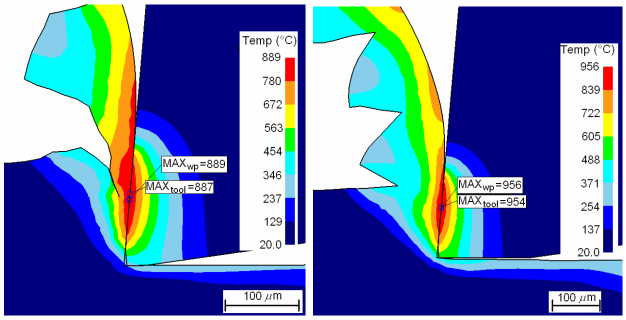

Deform: (c) VB = 0.03mm; (d) VB = 0.20mm.

Fig. 7: Temperature distribution at the tool-chip-workpiece interfaces.

In addition, both Deform and Abaqus show max temperature increase when tool with higher flank wear is used. In contrast with these similarities between the two software, Deform shows

higher max temperatures in both tool and chip. The reason is once again related to the different interface thermal model and heat global exchange coefficient at the tool chip interface, as well as to the different friction and material model implemented.

Finally, it can be noted that in any case the maximum temperature in the workpiece is lower than 980°C during the machining process, therefore no phase transformations are presented. Such evidence justifies the assumption to neglected phase transformation model in the material thermal, mechanical and physical properties in both the software.

Residual stress distribution considering tool wear. To consider the effect of successive cutting sequences on residual stress distribution, the physical state from the first cut is saved and used as initial condition for the second one. Other cutting conditions of the second cut are the same as those of the first cut. As concerned Abaqus procedure, in order to predict residual stress, three unloading steps were implemented at the end of each cut in this study: (1) Release the cutting forces, (2) release the clamping forces, and (3) release the workpiece to room temperature.

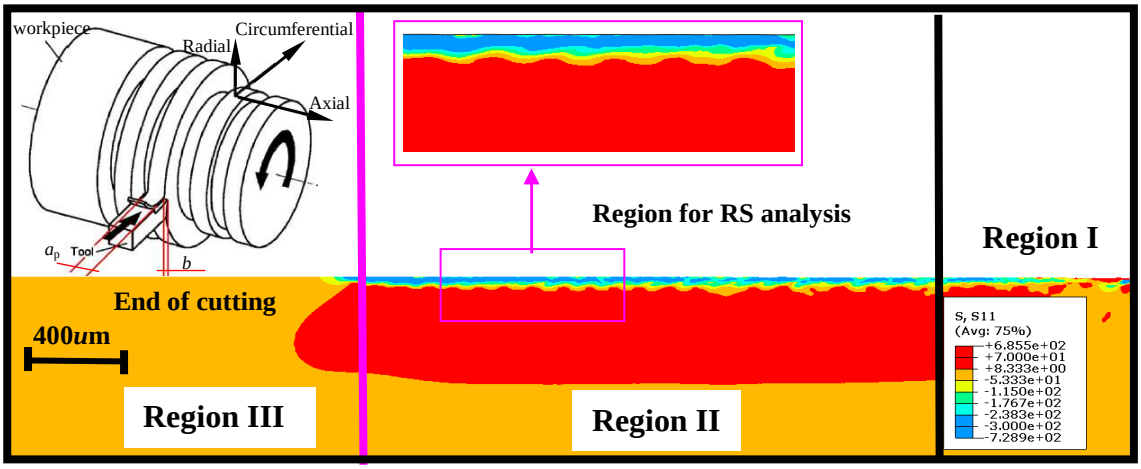

Fig. 8: Residual stress distribution on the workpiece.

After external force release and cooling down to room temperature, the final residual stress distribution on the workpiece is shown in Fig. 8. The stresses in Region II are selected to evaluate the residual stresses, and the predicted residual stresses should be also averaged over the same volume and the mean value should be taken. The oscillated residual stresses caused by the segmented chip are observed on the machined surface, which present the microstructure of the machined surface.

Vice versa, as far as Deform procedure since an automatic method for residual stress collection is not yet implemented in SFTC-DEFORM-2D® V.10, the following procedure was employed: (1) for several time steps, the tool was released from the machined surface (unloading phase) and the workpiece was cooled down to the room temperature; (2) residual stress profiles at several locations (coincident to Region II, Fig. 9) of the machined surface were collected and the average values were calculated, as described in [23].

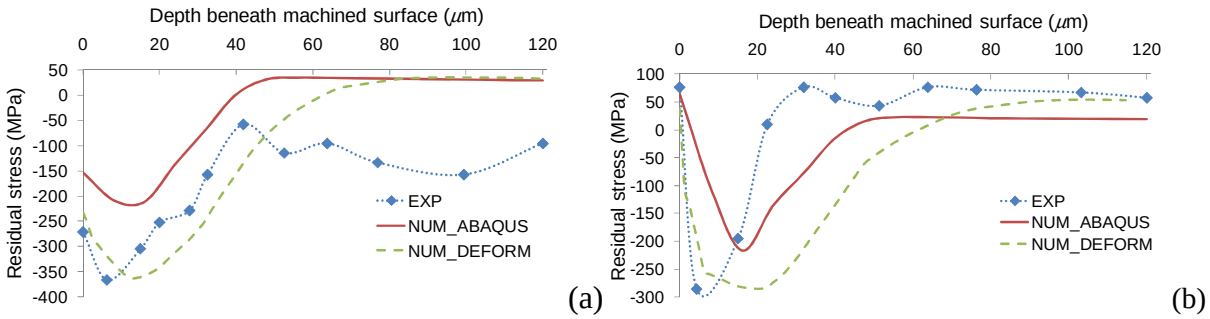

Fig. 9: Effect of the flank wear length on circumferential residual stress profile: (a) VB = 0.03mm; (b) VB = 0.2mm

Fig. 9 shows the effect of flank wear length on residual stress distribution beneath the newly machined surface, the acquired experimental ones are also detailed in Fig. 8 from literature [13]. As general trends, both the software highlight that when the flank wear was increased from 0.03 to 0.2 mm, the surface residual stress towards the tensile region. This is due to the higher magnitude of temperature generated along flank face/work piece interface.

Moreover, both Deform and Abaqus show that either the maximum compressive residual stress as well as the beneficial depth decreasing with increasing of flank wear. In addition, the distance where maximum compressive residual stress is located seems to be not affected by flank wear. What's more is that Deform shows a better numerical residual stress prediction compared to Abaqus, especially in the 20-40 μm below the machined surface. However, both the software show some gap between experiments and simulations, also considering the influence of first cut. The reason of such discrepancy should be related to firstly the material flow stresses used in both Abaqus and Deform which are not suitable to describe the metallurgical material states; secondly, It is worth to point out that in both the calculations, the residual stresses due to phase transformation were neglected and, especially in the case of Deform (temperature near to phase transformation effect), such assumption is not properly corrected.

Conclusions

In this study, a comparison of three group simulations performed with two different 2D FE models is presented for the Ti-6Al-4V alloy, and the simulation results are compared with experimental values.

Some observations concerning the results obtained based on the two codes are presented in the following points:

- The present work demonstrates that serrated chip formation can be modelled using the mentioned two codes with appropriate material and damage models.
- The temperature distribution at the tool-chip-workpiece interfaces displays that the segmentation is the result of fracture phenomenon (Defortm and Abaqus) and the coexisting a thermal softening state (Abaqus).
- The simulation results of temperature and residual stress along the depth beneath the machined surface show the similar tendency for two kinds of models, even though there is some gap between them, which is due to the optimal conditions for each of them in terms of material laws, damage criteria, etc.
- Potentially, this benchmark model can be exploited to perform other numerical comparisons with both commercial and in-house codes.

Acknowledgments

The authors of LaMCoS laboratory would like to acknowledge the financial support of China Scholarship Council (CSC).

References

[1] T. Mabrouki, F. Girardin, M. Asad, and J.F. Rigal: Int. J. Mach. Tools Manuf. 48 (2008), p. 1187-1197

[2] D. Umbrello, J.C. Outeiro, R.M. Saoubi, A.D. Jayal, and I.S. Jawahir: CIRP Annals - Manufacturing Technology. 59 (2010), p. 113-116

[3] E. Usui, T. Shirakashi, in: *Proceedings of the first international conference on production engineering. Part I* (1974), p 535-540

[4] R. Gandikota, V.A. Madhavan, and V. Agarwal: AIAA Journal. 38(2000), p. 2176-2186

[5] E. Merchant: Transaction of the ASME, Jour. App. Mech. 66 (1944), p. 168-175

[6] P.J. Arrazola, D. Ugarte, J. Montoya, A. Villar, and S. Marya, in: *VIII International Conference on Computational Plasticity COMPLAS VIII*, Barcelona (2005)

[7] L. Deshayes, R. Ivester, T. Mabrouki, and J.F. Rigal, in: *Proceedings of IMECE*, November 13-20, Anaheim, California, USA (2004)

[8] J. Soriano, I. Llanos, T. Özel, P.J. Arrazola, In: *12th Cirp Conference on Modelling of Machining Operations*, Donostia San Sebastián, Spain, May 7-8 (2009)

[9] J.C. Williams, G. Lutjering: *Titanium*. Springer – Verlag (2003)

[10] Information on http://www.matweb.com

[11] K.C. Mills: *Recommended values of thermo physical properties for selected commercial alloys*, Abington Hall, Abington, Cambridge, Woodhead Publishing Limited (2002)

[12] G.R. Johnson, W.H. Cook, In: *Proceedings of the 7th international symposium on ballistics*, the Hague, (1983) p. 31-48

[13] L. Chen, T.I. El-Wardany, and W.C. Harris: CIRP Annals - Manufacturing Technology, 53 (2004) p. 95-98

[14] A. Hillerborga, M. Modéera, and P.E. Petersson: Analysis of crack formation and crack growth in concrete by means of fracture mechanics and finite elements, Cement and concrete research, 6 (1976), p. 773-782

[15] K.L. Johnson: *Contact mechanics*, Cambridge university press, Cambridge (1985)

[16] T. Mabrouki, J.F. Rigal: Journal of Materials Processing Technology, 176 (2006), p. 214-221

[17] Deform®-User Manual. SFTC-Deform V10.0.2, Columbus (OH), USA (2010)

[18] M.G. Cockroft, D.J. Latham: J. Inst. Met. 96 (1968), p. 33-39

[19] Y.C. Yen: Modeling of metal cutting and ball burnishing – Prediction of tool wear and surface properties, PhD Dissertation, Ohio State University (2004)

[20] D. Umbrello: Journal of Materials Processing Technology, 196 (2008), p. 79-87

[21] H. Jiang, R. Shivpuri: Journal of Materials Processing Technology, 150 (2004), p. 124-133

[22] M. Calamaz, D. Coupard, and F. Girot: International Journal of Machine Tools and Manufacture, 48 (2008), p. 275–288

[23] C.R. Liu, Y.B. Guo: International Journal of Mechanical Sciences, 42 (2000), p. 1069-1086